

Complex Made from Tetrasodium *N*,*N*-Bis(carboxylatomethyl) Glutamate and Sodium Oleate that Forms a Highly Ordered Lamella in Gel Phase

Yeonhwan Jeong,[1] Kazuya Uezu,[1] Masataka Kobayashi,[2] Shinichi Sakurai,[3] Hiroyasu Masunaga,[4] Katuaki Inoue,[4] Sono Sasaki,[4] Naohiko Shimada,[1] Yoichi Takeda,[1] Kenji Kaneko,[5] and Kazuo Sakurai*[1]

[1]Department of Chemical Processes and Environments, The University of Kitakyushu, 1-1 Hibikino, Wakamatsu-ku, Kitakyushu 808-0135

[2]Laboratory SHABONDAMA SOAP Co., Ltd., 23-1, Minamifutajima 2-chome, Wakamatsu-ku, Kitakyushu 808-0135

[3]Department of Polymer Science and Engineering, Kyoto Institute of Technology, Matsugasaki, Kyoto 606-8585

[4]SPring-8, Japan Synchrotron Radiation Research Institute (JASRI), 323-3 Mihara, Mikazuki, Sayo-gun, Hyogo 679-5198

[5]Department of Material Science and Engineering, Graduate School of Engineering, Kyushu University, 744 Motooka, Nishi-ku, Fukuoka 819-0395

Received February 27, 2006; E-mail: sakurai@env.kitakyu-u.ac.jp

When we mixed two transparent aqueous solutions of tetrasodium *N*,*N*-bis(carboxylatomethyl) glutamate (GLDA) and sodium oleate (OleNa), a white gel phase was formed when the total solute concentrations were higher than about 2.8 wt %, indicating that complexation between GLDA and OleNa caused the gelation. The appearance of the gel was completely opaque, the gel displayed thixotropy, and the gel state changed to the sol state upon heating. Optical microscopy showed that the gel consisted of very long fibers with diameters ranging from nanometers to micrometers. Transmission electron microscopy showed that the long fibers were made from many bundled, straight fibrils with a width of 200–1000 nm. The fibril consisted of lamellae parallel to the axial direction of the fibril. X-ray scattering confirmed the lamellar structure with a spacing of 4.5 nm, and the spacing was independent of the concentration and the molar ratio of GLDA and OleNa. The area of the lamellar first peak reached a maximum at the molar ratio of GLDA:OleNa = 4:1, i.e., this ratio is the stoichiometry of the GLDA/OleNa complex. This stoichiometric number was confirmed by high-performance liquid chromatography.

Surfactants can self-assemble to form a variety of different micellar structures in aqueous solutions. The driving force of the self-assembling process can be ascribed to tendency of the molecules to avoid unfavorable interactions between their hydrophobic parts and water (hydrophobic interactions). In the self-assembling process, the molecules aggregate together to form micelles, in which the hydrophilic headgroups (generally ionic groups) point outwards in contact with water, and the hydrophilic tails point inwards away from the water medium. One of the key factors that determine the micellar structures is repulsion between the hydrophilic head groups. At low surfactant concentrations or low ionic strengths, the head groups try to separate as far as possible, which leads to spherical micelles. In the case of the higher surfactant concentration or the higher ionic strength, the micelles form a disc- or rod-like architecture. In the region of the phase diagram called "cylinder phase," the micelles have stretched into threads or columns that pack in a hexagonal array. At the far higher concentrations, the micelles have flattened into sheets or lamellae.

Sodium oleate (OleNa) is one of the most widely used surfactants, and has many uses, such as food additives, an ingredient of shampoos and detergents, and cooking oils. The phase behavior of the aqueous solution of OleNa has been studied by many researchers.[1–7] The first attempt to construct the phase diagram was made in 1939.[2] According to the established diagram, OleNa is not soluble in water and forms spherical micelles at low concentrations. In the range of 25–50 wt %, it forms a cylinder phase and at >50 wt %, a lamellar phase appeared.

Recently, addition of the third component to the OleNa/water system has gained attention because it is possible to control the phase behavior and the micellar structures. Watanabe et al.[8] found a novel stable vesicle and sponge phases by adding a mixed surfactant system to oleic acid. Gradzielski et al.[9–11] found a very stiff gel phase in the OleNa/1-octanol/water ternary system. For sufficiently high 1-octanol content, vesicles that are formed are so monodisperse that they are able to form a densely packed system with long-range order and with a shear modulus that is about 100 times higher than normally found for vesicle systems. This was the first system of this type that forms a cubic-phase-like arrangement of monodisperse vesicles. They called their system "vesicle gels."

Published on the web February 13, 2007; doi:10.1246/bcsj.80.410

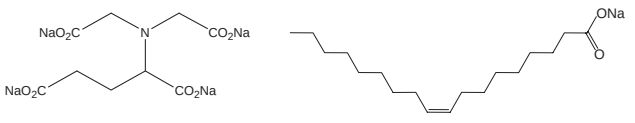

GLDA OleNa

Fig. 1. Chemical structures of the gelators: tetrasodium *N*,*N*-bis(carboxylatomethyl) glutamate (GLDA) and sodium oleate (OleNa).

While some amphiphilic molecules can gelatinize water,[12–15] others can gelatinize organic solvents, and these systems are called "organogels."[16–26] In organogels, the molecules self-assemble to form a very long cylindrical fiber, and the fibers are entangled to form networks that can absorb a large amount of solvent. In this paper, we report a "SAFIN (Self-assembled fibrillar network) gel"[27] made from tetrasodium *N*,*N*-bis(carboxylatomethyl) glutamate (GLDA) (see Fig. 1) and OleNa in relatively dilute aqueous solutions. GLDA is a chelating agent, and to the best of our knowledge, there have been no reports about aqueous gels made from OleNa and chelating agents.

Experimental

Samples and Gelation Test. Tetrasodium *N*,*N*-bis(carboxylatomethyl) glutamate (GLDA) and sodium oleate (OleNa) were purchased from TCI chemicals, Japan and used without further purification. An aqueous GLDA solution was added to an OleNa solution and mixed for a few minutes to form a gel. pH Measurement was performed with a HORIBA pH meter (Japan) after calibration with buffer solutions of pH = 4, 7, and 10. The pH of the GLDA solutions at 3.4 and 6.8 wt % was about 12. The pH of OleNa aqueous solutions at 3.4 and 6.8 wt % was about 10. The pH of the GLDA/OleNa mixtures was 11.3–12.5.

Turbidity was measured in the range of 800–610 nm with a JASCO UV spectrometer to examine the gelation and stoichiometry. DSC measurements were performed with a Perkin-Elmer Pyris1. A given amount of the gel was placed in an aluminum pan, and the pan was mechanically sealed. The pan was heated at a scanning rate of $10\,^{\circ}\mathrm{C\,min^{-1}}$.

Optical and Electron Microscopic Observations and Mapping of Nitrogen and Sodium. Optical polarizing microscopy (OPM) was carried out with a Nikon ECLIPSE E6003 at room temperature. Transmission electron microscopy (TEM) and high-resolution TEM (HRTEM) images were acquired using a JEOL TEM-2010 (accelerating voltage 200 kV) and a TECNAI-20, FEI (accelerating voltage 120 kV), respectively. The gel was placed on a copper TEM grid (200 meshes) with a holey carbon support film. TEM grid was freeze-dried overnight and, if necessary, stained with osmium tetroxide vapor for 10 min. The TEM grid was dried at room temperature in vacuum for 12 h before TEM observation.

X-ray Scattering Experiments. For the scattering experiments, we prepared the GLDA/OleNa mixtures with the total solute concentrations of 0.9, 2.8, 3.4, and 6.8 wt % with different mixing ratios. The samples were loaded into a quartz cell (Mark-Röhrchen) with 2 mm diameter, and then, the cell was sealed with an epoxy adhesive.

Wide-angle X-ray scattering (WAXS) were performed at the BL40B2 station at SPring-8 and in the Instrumental center at the University of Kitakyushu in Japan. With a Rigaku XRD-DSC-II, WAXS data was accumulated with a slit width of 0.15 mm at a scanning speed of $0.02^{\circ}\,\mathrm{min^{-1}}$ in the scattering angle range of $2\theta = 2$–30° at room temperature. Small-angle X-ray scattering (SAXS) experiments were carried out at the BL40B2 station at SPring-8 in Japan, where the camera-length and the X-ray wavelength were adjusted to 150 cm and 1.0 or 1.5 Å, respectively.[28,29] In the scattering experiment, the beam size was 0.1×0.1 mm at the sample position, and the sample thickness was 2 mm. The scattering intensity was accumulated for 300 s in the range of $q = 0.08$–$6.7\,\mathrm{nm^{-1}}$ with a Rigaku R-AXIS IV++ system (a $30\,\mathrm{cm} \times 30\,\mathrm{cm}$ imaging plate), where q is the magnitude of the scattering vector defined by Eq. 1.

$$q = \left(\frac{4\pi}{\lambda}\right)\sin\left(\frac{\theta}{2}\right), \tag{1}$$

where λ is the wavelength of X-ray radiation and θ is the scattering angle.

High-Performance Liquid Chromatography. Six samples with concentration of 3.4 wt % and molar ratios of GLDA:OleNa from 1:1 to 6:1 were prepared and centrifuged at 3000 rpm at 20 °C to separate the supernatant. The supernatants were filtered through a PTFE membrane with 0.2 μm pore size (ADVANTEC Co.) and diluted by 100 times with distilled water. The solutions were forced to flow through a YMC-Pack ODS-AQ column (YMC Co., Ltd., Japan) at 25 °C with a gradient mobile-phase composition; the mobile-phase composition was changed from 0.01 M trifluoroacetic acid/water solution to 0.01 M trifluoroacetic acid/methanol. GLDA was detected by using its UV absorbance at 250 nm, and the concentration in the supernatant was determined at this absorbance. Because of micelle formation or aggregation of OleNa, there were many peaks corresponding to OleNa in the HPLC chart, and thus, it was difficult to determine the concentration of OleNa. On the other hand, GLDA gave clear peaks in the chromatogram.

Results

Gelation, Thixotropy, and Phase Diagram of the GLDA/OleNa Mixtures in Aqueous Solutions. OleNa and other fatty acids, which are transparent in solution, form spherical or cylindrical micelles at relatively low concentrations (typically < 500 mM).[1–3] When GLDA and OleNa aqueous solutions were mixed, after a few hours (depending on the concentration and composition), gelation took place and, in some cases, the entire solution became white and opaque. Figure 2 shows the typical changes in appearance during this gelation process. When we mixed GLDA and OleNa in an aqueous solution (1:1 in molar ratio, the total solute concentration was 110 mM), the solution became partially opaque (Fig. 2b). Vigorous stirring of the solution for a few minutes gave a large amount of bubbles and a transparent solution (Fig. 2c). When the mixed solution was left at room temperature, the bubbles gradually decreased, and the solution became turbid. After 10 h, the entire solution became white and opaque (Fig. 2d). When the vial was slowly turned upside down, the white material (or fluid) did not fall down because the gelation had already taken place, and the material completely lost fluidity (Fig. 2e). It took more than ten hours to complete the gelation, which is shown in the Supporting Information (Fig. S1). When we vibrated the fluid for a few minutes with a handy vortex shaker, it became solution again and the appearance became partially transparent (Fig. 2f). The process of (f)→(c)→(d)→(e)→(f) can be repeated many times. The feature presented in Fig. 2 is typical

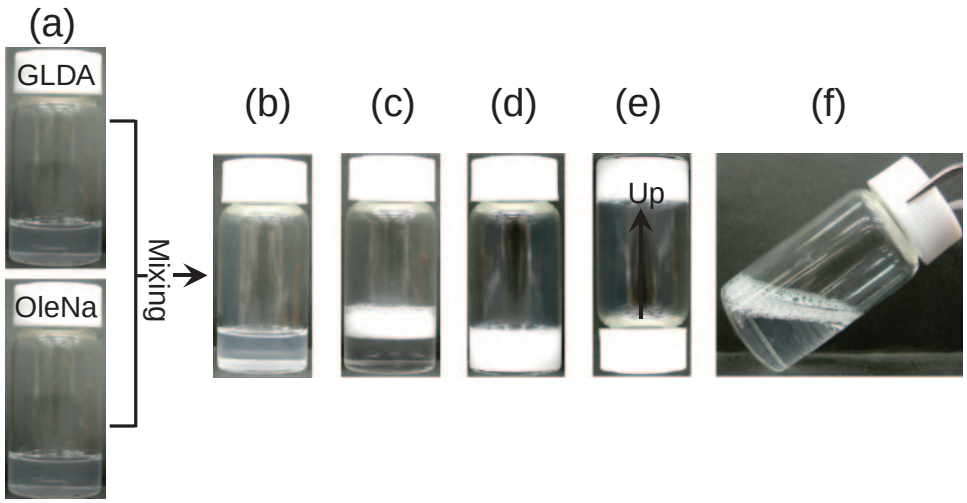

Fig. 2. Photographs to show how the gelation took place when GLDA and OleNa were mixed. The total solute concentration was 3.4 wt %, and the molar ratio of GLDA:OleNa was 1:1. (a) Before mixing, (b) just after mixing, (c) after stirring the mixture with a vortex for a few minutes, (d) after left at room temperature for 10 h, (e) when the sample vial of (d) was turned upside down, (f) after shaking the vial with a handy vortex.

for thixotropy. The appearance of thixotropy indicates that weak intermolecular interactions build relatively large structures in the fluid. It should be noted that gelation and thixotropy were observed only for the GLDA/OleNa aqueous mixtures.

The phase diagram for the ternary system, i.e., OleNa, GLDA, and water, at 25 °C and pH = 11.3–12.5 was constructed (Fig. 3) by judging whether the gelation took place on the basis of the appearance of the sample that had been left at 25 °C for 10 h. When the entire solution became white and lost fluidity, we classified it as being in the gel phase. When we saw a small amount of gel-like precipitation, we classified it as two-phase. On the other hand, turbid solutions without precipitation were classified it as being in the sol state. The gelation region appears when the total solute concentration exceeds 83 mM (2.8 wt %). Based on the previous work,[3] OleNa forms spherical micelles at this concentration. As shown later, GLDA never form aggregates in the concentrations studied in Fig. 3. Therefore, the appearance of the gel is ascribed to synergistic effect brought by the mixture of OleNa and GLDA, presumably due to the formation of a complex between OleNa and GLDA.

GLDA has four carboxylate groups with chemical structure similar to that of ethylenediaminetetraacetic acid (EDTA). Therefore, GLDA can act as a chelating agent for calcium and magnesium cations. When we added $CaCl_2$ to the GLDA/OleNa gel (3.4 wt %, 1:1 in mol), the gel changed to the sol state. Furthermore, when HCl was added to the gel so that the solution had a pH 1.2, the gel became a transparent sol. These phenomena suggest that the carboxylate groups in GLDA are involved in the formation of the gel. Thus, we examined whether EDTA forms a similar gel when it was mixed with OleNa; however, no gelation occurred. This comparison shows that the gelation is a unique property of GLDA.

Morphology of GLDA/OleNa Gels with Optical and Electron Microscopy. In Fig. 4a, which shows the optical microscopic images for a 110 mM gel (3.4 wt %, 1:1 in mol),

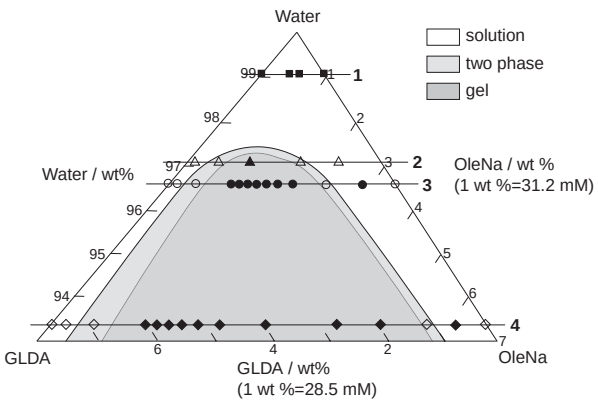

Fig. 3. Phase diagram for three component system of GLDA/OleNa/water, constructed on the basis of the appearance after 10 h at 25 °C. In the phase diagram, the light gray region represents the two phase region (white aggregates and transparent solution), the dark gray region is the gel phase (gel), and white region is solution phase (sol). Four lines in the diagram stand for the region where SAXS measurements and optical polarizing microscopy were performed. Line 1 is at a total solute concentration of 0.9 wt % (squares), line 2 is at a total solute concentration of 2.8 wt % (triangles), line 3 is at a total solute concentration of 3.4 wt % (circles), and line 4 is at a total solute concentration of 6.8 wt % (diamonds). Dark squares, triangles, circles, and diamonds indicate the points at which SAXS experiments were performed. Mixed samples of GLDA and OleNa were put down at room temperature for 10 h, and then, the appearances of samples were observed.

very long fibers with the diameters ranging from micrometers to nanometers can be seen. In the cross polarization mode (Fig. 4b), there is no strong birefringence, suggesting that the aggregates in the gels are not in the crystalline state. Sometimes, weak birefringence was observed (indicated by

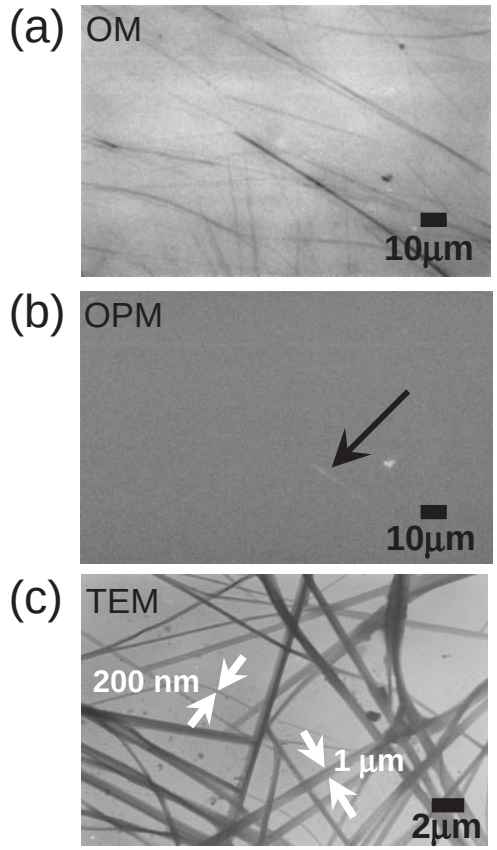

Fig. 4. Optical microscopy (OM) (a) and optical polarizing microscopy (OPM) with cross polarization (b) of 3.4 wt % gel (G:O = 1:1), and transmission electron microscopy (TEM) images (c) of 3.4 wt % gel (G:O = 4:1). TEM image of a gel shows very long tapes with a diameter of 200–1000 nm. TEM grids were not stained with osmium tetraoxide vapor. An arrow in panel (b) denotes weak birefringence.

the arrow), which can be ascribed to the fact that the molecules are highly oriented. When we increased the concentration to 220 mM (6.8 wt %), we could see more birefringence than that in Fig. 4b, probably because highly ordered structures are formed. We confirmed that crystallization did not occur at this concentration with WAXS measurements.

Figure 4c shows a typical TEM image for the GLDA/OleNa gels. There are many long straight fibrils with widths of 200–1000 nm, and these fibrils are connected to each other by junction points. The wider fibrils seem to consist of the narrow ones and the wider fibrils are bound together to form very wide and large fibers; therefore, the large fibers observed with optical microscopy are bundles of these fibrils in Fig. 4c. The network structure presented in Fig. 4c must be responsible for the gelation of the GLDA/OleNa mixtures. The bundled fibers and the presence of junction points are similar to the morphology of organogels but different from the vesicle gels found by Gradzielski et al.[10] Here, the molar ratio (GLDA:OleNa = 4:1) was the stoichiometric ratio of the complex, and the total solute concentration was 3.4 wt %. When we made a sample with an off-stoichiometric ratio, dots were observed in TEM image. These dots are probably un-complexed material deposited on the TEM grid during the freeze-drying process. The gel undergoes gel-to-sol transition at 33.1 °C (Fig. S2 in Supporting Information). When we carried out the freeze-drying treatment above 35 °C, we observed no fibril, but many dots.

The double bond of OleNa is stainable with osmium tetraoxide, providing a contrast for TEM. Figures 5a and 5b show a TEM image of a stained sample of the GLDA/OleNa gel. The magnified image in Fig. 5b shows that a lamellar structure is present in the fibril, the spacing of the lamellae is about 3.6 nm, and the lamellae are parallel to the axial direction of the fibril. The absolute value of the spacing might contain some experimental error owing to titling of the sample or focusing problems, while the lamellar structure that extends parallel to the axial direction was reproducible. It should be mentioned that the presence of the lamellae and the size of the spacing are similar to those of the pure OleNa solid. Figure 5c shows another TEM image of the GLDA/OleNa gel without staining and the thick solid line indicates the section where electron dispersive X-ray spectroscopy (EDX) was measured for N and Na atoms. The resultant EDX profiles (Fig. 5d) show that the fibril contains nitrogen atoms at the almost same position as that of sodium. Since the origin of the nitrogen atom is ascribed to the amines of GLDA, we can conclude that the fibril contains both GLDA and OleNa molecules. Therefore, the lamellar structure in Fig. 5b is made from both GLDA and OleNa.

X-ray Scattering. Figure 6 compares the scattering profiles between the GLDA/OleNa gel (2.8 wt %, GLDA:OleNa = 4:1) and a solid sample of OleNa. Both samples have clear Bragg's diffraction peaks up to the 7th order (6th peak becomes weak due to the extinction rule of X-ray diffraction). The peak positions completely satisfy the ratio expected for lamellae, and the spacing values of the gel and the solid were determined to be about 4.4 and 4.5 nm, respectively. The measurements were carefully performed for the OleNa solid and the GLDA/OleNa gel at the same camera length and the same wavelength for several repetations so that the results could be compared. The results always showed that the spacing of the gel was larger than that of the OleNa solid. For both samples, the even-numbered peaks show lower height than that of the odd-numbered peaks, indicating that the thickness ratio of the two layers in the lamellar structures is close to 0.5.[30] When the peak heights were compared quantitatively (Table 1), the even-numbered peak of the solid sample was relatively larger than that of the gel sample. This difference suggests that the layer structure is different between the gel and the solid, and the thicknesses of the two layers in the gel are close to being equivalent to the solid.[30] One might consider that the lamellar structure in the gel can be ascribed to OleNa crystals that were formed, somehow, by adding GLDA to OleNa solutions. However, this argument does not hold, because the difference in the spacing is greater than the experimental error, as shown in the inset of the figure, and the thickness ratio of the two lamellar layers is different. In addition, the solid sample has clear crystalline peaks around $2\theta = 15°$, and the peaks are smeared owing to polymorphism. On the other hand, the gel has no such peaks in this region. The very broad groundswell of the base line and the small peaks around $2\theta = 15°$ may be ascribed to the amorphous nature of the GLDA/OleNa gel, similar to

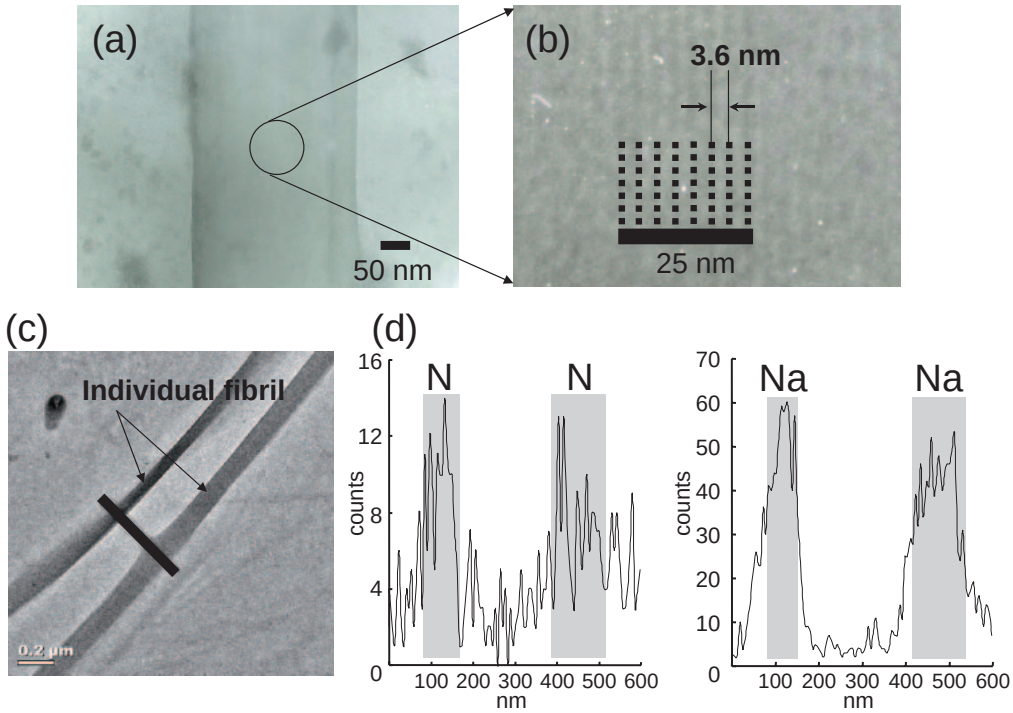

Fig. 5. TEM images and EDX line profiles of 3.4 wt % gel (freeze-dried sample). TEM specimens were dried for 12 h. The specimen (a) was stained with vapor of 0.1% osmium tetraoxide aqueous solution for 10 min and specimen (c) was unstained. The magnified image (b) of (a) shows a lamellar spacing of 3.6 nm parallel to the axial direction of the fibril. The thick line in image (c) denotes the section where EDX was measured for the N and Na atoms. The scale bar in (c) corresponds to 200 nm. Panel (d) shows EDX line profiles for N and Na atoms.

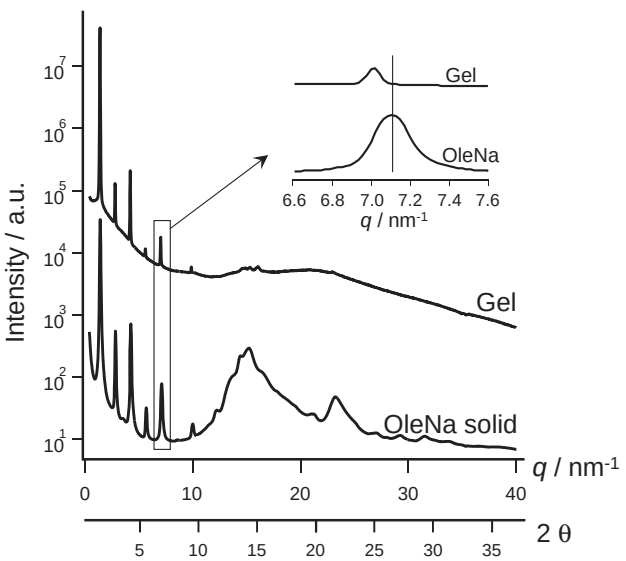

Fig. 6. Comparison of the X-ray scattering profiles between 2.8 wt % gel (GLDA:OleNa = 4:1) and OleNa solid. The inset is the magnified profile of the 1st and 5th peaks of both gel and OleNa solid. Background scatterings from water solvent and air were subtracted.

other organized systems.[31–33]

Figure 7 shows plots of the scattering profiles as a function of the GLDA/OleNa molar ratio with a fixed total solute concentration of 6.8 wt % (in relation to the line 4 in Fig. 3 with measurements made at the marked points). The GLDA solution has no peaks, except for up-turn in the smaller q region,

Table 1. Comparison of Peak Height Ratios of Gel and Solid

	Gel	Solid
2nd/1st	0.23	0.50
4th/3rd	0.08	0.30

which means that the GLDA molecules do not form any ordered structures but form random aggregates. On the other hand, the OleNa solution shows a broad peak at $q = 0.5$–2.0 nm^{-1}, which is ascribed to particle scattering from micelles. When we mixed GLDA and OleNa at a ratio of 1:17, the mixture was in the sol state, as shown in Fig. 3, and the scattering profile of this sample showed the presence of micelles. By comparing the profiles between 1:17 and OleNa, the addition of GLDA to OleNa induces dramatic changes in the micelle structure. Once the GLDA/OleNa composition reached the gel region, see Fig. 3, lamellar peaks appeared. It is interesting that the positions of the peaks are independent of the composition. When we carried out the same experiment at 3.4 wt % (Fig. S3 in the Supporting Information), the peak positions were the same as those of the 6.8 wt % gels, indicating that the lamellar spacing in the gel does not depend on either the GLDA/OleNa composition or the total solute concentration. This feature suggests the formation of a stoichiometric complex between GLDA and OleNa. We carried out further X-ray scattering experiment at concentrations of 0.9 and 2.8 wt %. At 0.9 wt %, no gel formed, and the scattering profiles always showed the presence of micelles (Fig. S4 in Supporting Information).

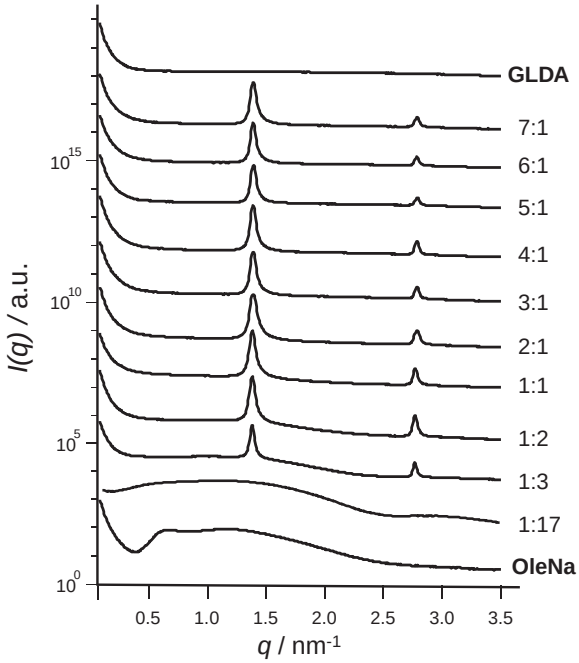

Fig. 7. GLDA:OleNa molar ratio dependence of SAXS measured at room temperature. The total solute concentration was fixed at 6.8 wt %.

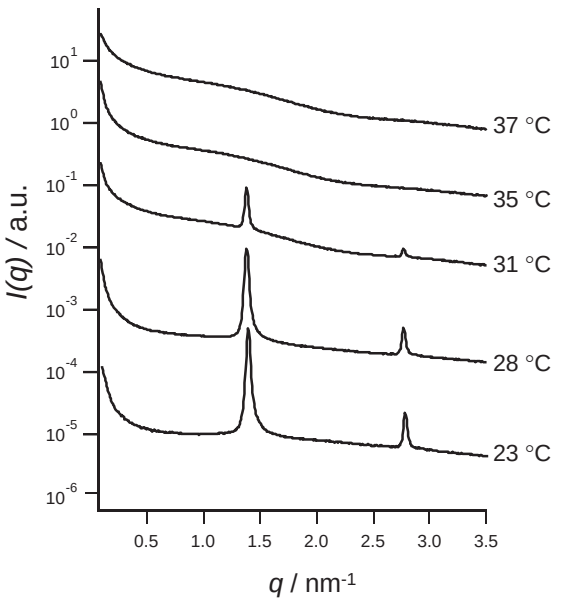

Fig. 8. Temperature dependence of SAXS profiles for 6.8 wt % total concentration at GLDA:OleNa = 4:1. Gel-to-sol transition temperature by DSC was 34.4 °C.

Figure 8 shows the temperature dependence of the lamellar peaks for the 6.8 wt % GLDA:OleNa = 4:1 sample; the gel-to-sol transition temperature was determined to be 34.4 °C by DSC (Fig. S2 in Supporting Information). Although the peak height decreases with increasing temperature, the position did not change, and above the transition temperature, the peak disappeared. In addition, the particle scattering from micelles remains. One peculiar feature of the GLDA/OleNa gel is that the lamellar spacing is even independent of temperature.

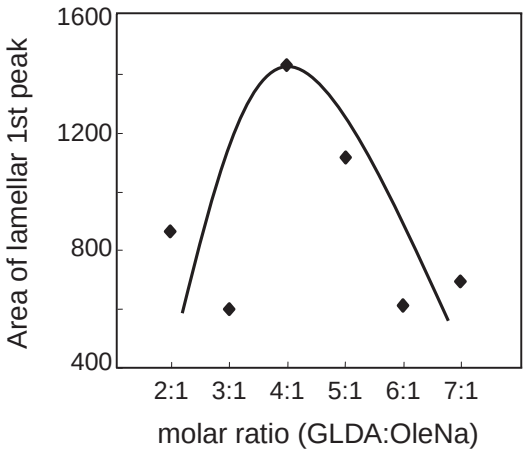

Fig. 9. GLDA:OleNa molar ratio dependence of the lamellar 1st peak areas for 3.4 wt % gels.

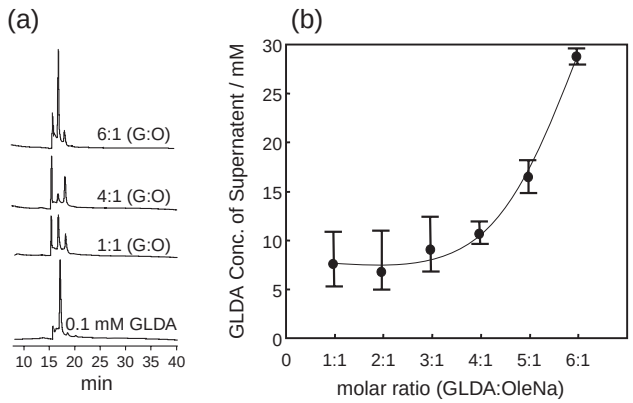

Fig. 10. HPLC elution profile (a) and GLDA:OleNa molar ratio dependence (b) of GLDA concentration in the supernatent solution. The supernatent solutions were diluted 100 times with distilled water and used to make a HPLC experiment.

Stoichiometry of the GLDA/OleNa Complex. We determined the stoichiometric ratio from X-ray scattering. When the solution was in the sol state, no lamellar peaks were observed. Therefore, the peak intensity can be related to the amount of the gel. Figure 9 shows plots the peak area of the first-order diffraction against the GLDA to OleNa molar ratio at 3.4 wt %, where the exposure time and the cell thickness were fixed and the scattering intensity was normalized by the incident X-ray intensity. There was an apparent maximum around GLDA: OleNa = 4:1, indicating that this is stoichiometric number of the complex, although there is large experimental error. There is a possibility that the scattering volume might be too small to overcome the inhomogeneity of the gels. The error becomes even larger for the 6.8 wt % samples, and this is the reason that Figure 9 was constructed for the 3.4 wt %.

Figure 10a shows typical HPLC charts for the supernatants of three samples (GLDA:OleNa = 6:1, 4:1, and 1:1), and a pure GLDA solution for comparison. Due to the difference in the extent of protonation of GLDA, three HPLC peaks were observed. We integrated the peak area from 15 to 22 min and calculated the GLDA concentration in the supernatants. Figure 10b shows plots of the concentration against the molar

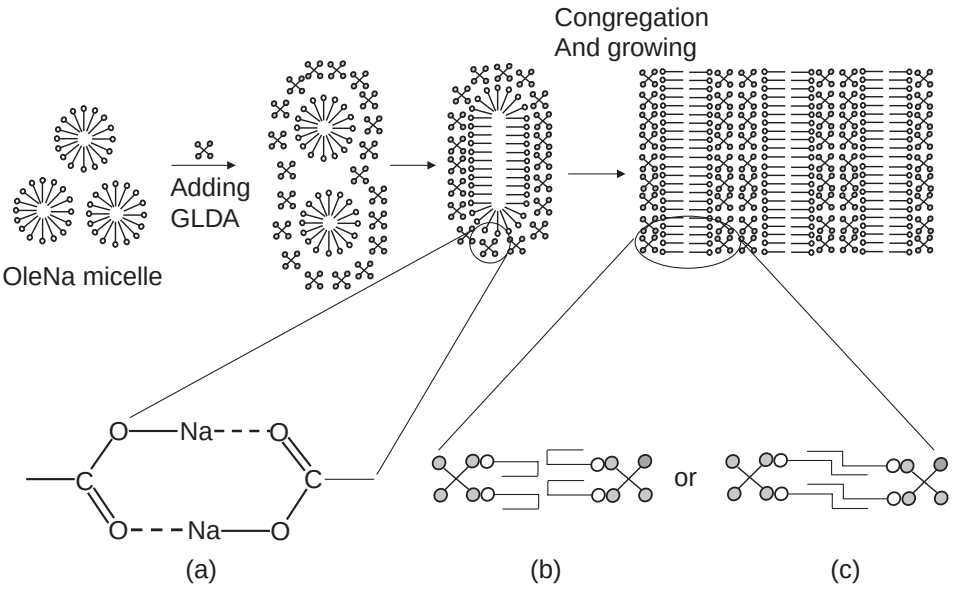

Fig. 11. Schematic of gelation mechanism by GLDA and OleNa: (a) sodium-bridging interaction, (b) U-shape without interaction, and (c) extended shape with interaction.

ratio (GLDA:OleNa). In the range of 1:1–4:1, the GLDA concentration changes little and increases with an increase in the molar ratio in the range of 4:1–6:1. This feature indicates that the extra amount of GLDA bleeds out of the gel phase into the supernatant when the molar ratio is larger than 4:1, which is consistent with the scattering results.

Discussion

Gelation Mechanism. X-ray scattering showed that OleNa itself forms micelles when the concentration is more than 0.9 wt %, which agrees with previous work.[3] The micelle formation of OleNa is driven by the hydrophobic attractions of the OleNa alkenyl chains. When GLDA was added to the micelles, the solution slowly became turbid. After a few hours or days, fibrils (Fig. 4) containing lamellae with a spacing of 4.5 nm were formed and the fibrils entangled with each other to form a network. This network is the reason that a gel state appears in the GLDA/OleNa mixture. The lamellae in the gel consist of both OleNa and GLDA. The question is how GLDA and OleNa interact with each other to form this structure.

Since de-protonated carboxylate groups on both OleNa and GLDA are essential for gelation, i.e., addition of HCl led the sol state, we can speculate that no hydrogen bonds are formed between the carboxylate groups of OleNa and GLDA. When we added $CaCl_2$ to the gel, the gel was destroyed, which implies that sodium cation is involved in the gelation, probably, by bridging between two carboxylate groups of OleNa and GLDA.[34–37] When we constructed a CPK model of GLDA, it was clear that the hydrophilic carboxylate groups cover the hydrophobic alkyl chain of GLDA, suggesting that GLDA cannot enter the hydrophobic layer formed by the OleNa alkenyl chains. Therefore, we conclude that the GLDA molecules exist in the water-rich phase and are connected with OleNa through sodium cations between both carboxylate groups, Fig. 11a (inset). Figure 11 shows a schematic of the gelation process. When two aqueous solutions of GLDA and OleNa are mixed, GLDA molecules come together around OleNa micelles to form a GLDA/OleNa complex through sodium-bridging interaction with the carboxylate groups. The complexes self-assemble with each other to become larger (Fig. 2c), leading to a long lamellar tape (Fig. 2d). After several hours, the process reaches equilibrium, and the lamellae entangle each other to form a gel (Fig. 2e).

Structure of the Lamella in the GLDA/OleNa Gel. Our scattering experiments showed that the lamellar spacing in the gel (4.5 nm) is slightly longer than that of the OleNa solid (4.4 nm). This similarity in the spacing is, in fact, surprising because the result means that the lamellar spacing does not change even after a large amount (4 times by molar) of GLDA molecules enter into the OleNa micelles. The crystal structure of oleic acid was reported by Ernst et al.,[38] and they concluded that oleic acid molecules are connected by hydrogen bonding between the carboxyl groups and the alkenyl chain in oleic acid, which has an extended form. The length of the extended form of oleic acid is about 1.9 nm. Therefore, the lamellar spacing of 4.4 nm of OleNa can be understood by assuming that two extended alkenyl chains face each other and are nested without interdigitation. This model is quite reasonable based on the crystal structures of stearic acid.[39] If OleNa takes the same extended conformation, the lamellar spacing in the gel would be much larger than that of the OleNa solid. The stoichiometric number suggests that two of the four carboxylate groups of GLDA interact with two OleNa molecules, Fig. 11. If this mode occurs, then the two carboxylate groups in GLDA would increase the packing distance between OleNa molecules. Once the packing distance is increased, the alkenyl chains can interdigitate with each other as shown in the inset of Fig. 11. Another possibility to accommodate the OleNa molecules is a "U-shaped conformation" as shown by in the same figure. This U-shaped model was proposed by Rich.[40] He found the low-energy conformers of oleic acid were generally U-shaped with the π-bonds located in the most curved

region of the loop. At this moment, however, we cannot fully rationalize the lamellar spacing in the gel state. Careful Raman spectral measurements[41] may help to determine the molecular structure of the lamellae in the gel.

Concluding Remarks

When we mixed two transparent aqueous solutions of GLDA and OleNa, a white gel phase formed. The gel was completely opaque, displayed thixotropy, and changed to a sol state upon heating. OM showed that the gel consisted of very long fibers with diameters ranging from micrometers to nanometers. TEM showed that the long fibers were made from many bundled straight fibrils with a width of 200–1000 nm. The fibril consisted of lamellae arranged parallel to the axial direction of the fibril. X-ray scattering confirmed the lamellar structure has a spacing of 4.5 nm, and the spacing was independent of the concentration and the molar ratio of GLDA and OleNa. The stoichiometry of the GLDA/OleNa complex was determined with X-ray diffraction and HPLC to be 4:1. The gelation mechanism was proposed, Fig. 11.

The synchrotron radiation experiments were performed at the BL40B2 in the SPring-8 with the approval of the Japan Synchrotron Radiation Research Institute (JASRI) (Proposal Nos. 2005A0680-NL2b-np, 2005A0681-NL2b-np, 2005B0150, and 2006A1581). XRD and TEM observation were carried out at the Instrumentation center of The University of Kitakyushu.

Supporting Information

Time dependence of the transmittance of 2.8 wt % mixed solution of GLDA and OleNa (GLDA:OleNa = 1:1) at room temperature (Fig. S1). DSC chart of 3.4 and 6.8 wt % gels (GLDA: OleNa = 4:1) (Fig. S2). Molar ratio dependence of GLDA and OleNa of SAXS profiles of total solute concentration of 3.4 wt % at room temperature (Fig. S3). SAXS profiles of solutions of total solute concentration of 0.9 wt % at room temperature (Fig. S4). This material is available free of charge on the web at http://www.csj.jp/journals/bcsj/.

References

1 P. A. Winsor, *Chem. Rev.* **1968**, *68*, 1.
2 J. Stauff, *Kolloid-Z.* **1939**, *89*, 224.
3 F. Reiss-Husson, V. Luzzati, *J. Phys. Chem.* **1964**, *68*, 3504.
4 V. Luzzati, F. Husson, *J. Cell Biol.* **1962**, *12*, 207.
5 D. P. Cistola, D. Atkinson, J. A. Hamilton, D. M. Small, *Biochemistry* **1986**, *25*, 2804.
6 H. Fukuda, A. Goto, H. Yoshioka, R. Goto, K. Morigaki, P. Walde, *Langmuir* **2001**, *17*, 4223.
7 K. Morigaki, P. Walde, *Langmuir* **2002**, *18*, 10509.
8 K. Watanabe, Y. Nakama, T. Yanaki, H. Hoffmann, *Langmuir* **2001**, *17*, 7219.
9 M. Gradzielski, M. Bergmeier, M. Muller, H. Hoffmann, *J. Phys. Chem. B* **1997**, *101*, 1719.
10 M. Gradzielski, M. Bergmeier, H. Hoffmann, M. Muller, I. Grillo, *J. Phys. Chem. B* **2000**, *104*, 11594.
11 M. Gradzielski, M. Muller, M. Bergmeier, H. Hoffmann, E. Hoinkis, *J. Phys. Chem. B* **1999**, *103*, 1416.
12 L. A. Estroff, A. D. Hamilton, *Chem. Rev.* **2004**, *104*, 1201.
13 M. de Loos, B. L. Feringa, J. H. van Esch, *Eur. J. Org. Chem.* **2005**, 3615.
14 M. Suzuki, M. Yamamoto, M. Kimura, H. Shirai, K. Hanabusa, *Chem. Lett.* **2004**, *33*, 1496.
15 M. Suzuki, M. Yamamoto, M. Kimura, H. Shirai, K. Hanabusa, *Chem. Eur. J.* **2003**, *9*, 348.
16 R. Oda, I. Huc, S. J. Candau, *Angew. Chem., Int. Ed.* **1998**, *37*, 2689.
17 P. Terech, G. Gebel, R. Ramasseul, *Langmuir* **1996**, *12*, 4321.
18 H. Engelkamp, S. Middelbeek, R. J. M. Nolte, *Science* **1999**, *284*, 785.
19 K. Yoza, N. Amanokura, Y. Ono, T. Akao, H. Shinmori, S. Shinkai, D. N. Reinhoudt, *Chem. Eur. J.* **1999**, *5*, 2722.
20 M. de Loos, J. van Esch, I. Stokroos, R. M. Kellogg, B. L. Feringa, *J. Am. Chem. Soc.* **1997**, *119*, 12675.
21 A. Ajayaghosh, S. J. George, V. K. Praveen, *Angew. Chem., Int. Ed.* **2003**, *42*, 332.
22 Y.-C. Lin, R. G. Weiss, *Macromolecules* **1987**, *20*, 414.
23 K. Hanabusa, M. Yamada, M. Kimura, H. Shirai, *Angew. Chem., Int. Ed. Engl.* **1996**, *35*, 1949.
24 P. Terech, R. G. Weiss, *Chem. Rev.* **1997**, *97*, 3133.
25 O. Gronwald, S. Shinkai, *Chem. Eur. J.* **2001**, *7*, 4328.
26 K. Murata, M. Aoki, T. Nishi, A. Ikeda, S. Shinkai, *J. Chem. Soc., Chem. Commun.* **1991**, 1715.
27 R. G. Weiss, P. Terech, *Molecular Gels, Materials with Self-Assembled Fibrillar Networks*, Springer, The Netherlands, **2006**.
28 T. Fujisawa, Y. Inoko, N. Yagi, *J. Synchrotron Radiat.* **1999**, *6*, 1106.
29 T. Fujisawa, K. Inoue, T. Oka, H. Iwamoto, T. Uruga, T. Kumasaka, Y. Inoko, N. Yagi, M. Yamamoto, T. Ueki, *J. Appl. Crystallogr.* **2000**, *33*, 797.
30 R.-J. Roe, *Methods of X-ray and Neutron Scattering in Polymer Science*, Oxford University Press, New York, **2000**.
31 K. Sakurai, Y. Jeong, K. Koumoto, A. Friggeri, O. Gronwald, S. Sakurai, S. Okamoto, K. Inoue, S. Shinkai, *Langmuir* **2003**, *19*, 8211.
32 Y. Jeong, K. Hanabusa, H. Masunaga, I. Akiba, K. Miyoshi, S. Sakurai, K. Sakurai, *Langmuir* **2005**, *21*, 586.
33 Y. Jeong, A. Friggeri, I. Akiba, H. Masunaga, K. Sakurai, S. Sakurai, S. Okamoto, K. Inoue, S. Shinkai, *J. Colloid Interface Sci.* **2005**, *283*, 113.
34 J. H. Dumbleton, T. R. Lomer, *Acta Crystallogr.* **1965**, *19*, 301.
35 G. C. Dismukes, *Chem. Rev.* **1996**, *96*, 2909.
36 B. Kersting, G. Steinfeld, *Inorg. Chem.* **2002**, *41*, 1140.
37 R. K. Hocking, T. W. Hambley, *Inorg. Chem.* **2003**, *42*, 2833.
38 J. Ernst, W. S. Sheldrick, J.-H. Fuhrhop, *Z. Naturforsch., B: Chem. Sci.* **1979**, *34*, 706.
39 *Kagaku Binran Kisoheiben II*, ed. by Nippon Kagakukai Hen, Maruzen Co., Ltd. Japan, **2000**, p. 706.
40 M. R. Rich, *Biochim. Biophys. Acta* **1993**, *1178*, 87.
41 P. Tandon, S. Raudenkolb, R. H. H. Neubert, W. Rettig, S. Wartewig, *Chem. Phys. Lipids* **2001**, *109*, 37.